JPNT 7(4), 267-275 (2018)
https://doi.org/10.11003/JPNT.2018.7.4.267

JPNT Journal of Positioning, Navigation, and Timing

Development of the KASS Multipath Assessment Tool

SungLyong Cho†, ByungSeok Lee, JongYeoun Choi, GiWook Nam

SBAS System Engineering & Integration Team, Korea Aerospace Research Institute, Daejeon 34133, Korea

ABSTRACT

The reference stations in a satellite-based augmentation system (SBAS) collect raw data from global navigation satellite system (GNSS) to generate correction and integrity information. The multipath signals degrade GNSS raw data quality and have adverse effects on the SBAS performance. The currently operating SBASs (WAAS and EGNOS, etc.) survey existing commercial equipment to perform multipath assessment around the antennas. For the multi-path assessment, signal power of GNSS and multipath at the MEDLL receiver of NovAtel were estimated and the results were replicated by a ratio of signal power estimated at NovAtel Multipath Assessment Tool (MAT). However, the same experiment environment used in existing systems cannot be configured in reference stations in Korean augmentation satellite system (KASS) due to the discontinued model of MAT and MEDLL receivers used in the existing systems. This paper proposes a test environment for multipath assessment around the antennas in KASS Multipath Assessment Tool (K-MAT) for multipath assessment. K-MAT estimates a multipath error contained in the code pseudorange using linear combination between the measurements and replicates the results through polar plot and histogram for multipath assessment using the estimated values.

Keywords: GPS, KASS, reference stations, multipath assessment, code pseudorange

1. INTRODUCTION

The Korea augmentation satellite system (KASS) provides correction and integrity information of global navigation satellite system (GNSS) to users through geostationary orbit satellites (Misra & Enge 2006). The ground infrastructure of KASS consists of KASS reference station (KRS), KASS processing station (KPS), KASS uplink station (KUS), and KASS control station (KCS). The KRS collects GNSS data and sends them to KPS through the network. The KPS calculates correction and integrity information using GNSS data and generates KASS messages (Yun et al. 2016). The KUS converts KASS messages to radio frequency (RF) signals using uplink antenna and sends the signals (Misra & Enge 2006). Users receive SBAS signals in KASS service area so that they can estimate accurate and safe location using correction and integrity information of SBAS message (Misra & Enge 2006).

Received Apr 24, 2018 **Revised** Sep 11, 2018 **Accepted** Oct 18, 2018
†**Corresponding Author**
E-mail: jackycho@kari.re.kr
Tel: +82-42-870-3999 Fax: +82-42-860-2789

The KASS performance (accuracy, integrity, availability, and continuity) is significantly affected by KRS site location and the collected GNSS raw data quality. The KASS performance at the system design phase is predicted assuming that the requirements of the reference station requirements are all satisfied. Thus, it is necessary to investigate KRS sites precisely that satisfy the site requirements to guarantee KASS performance at the system operation phase. For detailed KRS site investigation items, investigation of facilities for KRS equipment installation and operation (accessibility, security, fire and maintenance, etc.), Electro Magnetic Interference (EMI) for interference check of RF signals, and elevation and multipath assessment for the performance verification of GNSS raw data are essential (Cho et al. 2017). Among the investigation items, EMI and elevation can be verified precisely using existing or alternative equipment whereas multipath assessment requires new assessment measures due to discontinued existing equipment (Cho et al. 2017).

Since multipath signals have adverse effects on signal power and pseudorange of GNSS raw data received through antennas, analysis of multipath effects has been conducted in

http://www.ipnt.or.kr Print ISSN: 2288-8187 Online ISSN: 2289-0866

consideration of the adverse effect (Jakab & Townsend 2001). The signal power measurements are provided by MEDLL receivers, and a ratio between GNSS and multipath signal power (D/U: desired-to-undesired power ratio) was assessed. The pseudo range measurement assesses the multipath error estimate contained in GNSS code pseudorange measurement provided by commercial receivers. The multipath error can be estimated by removing errors (ionospheric delay, receiver noise, float ambiguity) contained in the code pseudo range measurement model (Weiss 2007).

This paper develops a KASS Multipath Assessment Tool (K-MAT) using multipath errors contained in the code pseudo range measurement due to the absence of alternative equipment and discontinued MEDLL receiver and MAT tool that provide signal intensity measurements. Chapter 2 discusses multipath signal characteristics and existing multipath assessment measures. Chapter 3 proposes an algorithm to estimate multipath error, and Chapter 4 implements a graphic user interface for output display and signal processing for multipath error estimation. Chapter 5 describes the implementation of K-MAT by a developer based on the design documents and verifies the functions through specification-based black box testing with regard to a channel (Khan 2011). In addition, the multipath effects are predicted from the surrounding geographic features around the antennas and compared with that of polar plot results for performance verification.

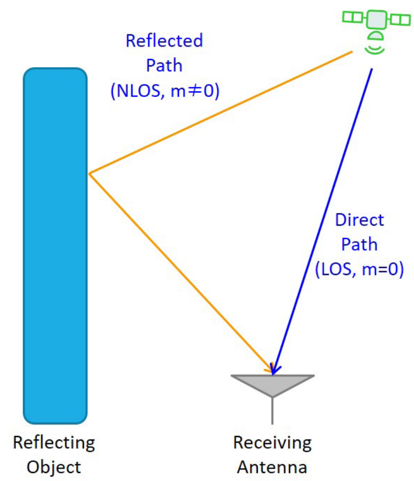

Fig. 1. Configuration of the receiving signal at the GPS antenna.

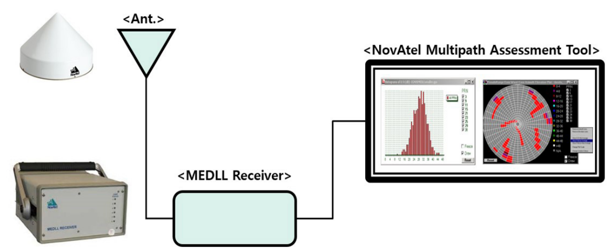

Fig. 2. Assessment environment of the multipath effect using the NovAtel's receiver and tool.

2. MULTIPATH SIGNAL CHARACTERISTICS

The global positioning system (GPS) signal consists of navigation message, code, and carrier phase. It is transmitted from satellites to receiver's antenna. The signal received at the antenna is composed of line-of-sight (LOS) signal, received directly from satellites, and non-LOS (NLOS) signal, reflected by the surrounding buildings, walls, or ground around the antennas (Townsend et al. 2000).

As shown in Fig. 1, signals received at the antennas are expressed by a sum of single LOS signal and multiple NLOS signals as presented in Eq. (1) (Townsend et al. 2000).

$$r(t) = \sum_{m=0}^{M-1} a_m p(t-\tau_m) \cos(\omega t + \theta_m) + n(t) \tag{1}$$

Here, m refers to the RF signal incident to the receiver from the same satellite, each of which has signal power (a_m). The signal p(t-τ_m) received at GPS receiver antenna is a code signal delayed as much as τ_m, a sinusoidal signal cos(ωt+θ_m) whose frequency is ω is a carrier phase signal delayed as much as θ_m, and n(t) is a receiver noise. The NLOS signal ($m \neq 0$) among various signals in Eq. (1) is a multipath signal, which degrades the performance due to the other code, and carrier phase delay.

The assessment of the multipath effects was presented as an important requirement to select GNSS antenna locations in monitoring or reference stations of existing GNSS, GBAS, and SBAS. For the assessment of the multipath effects to select existing sites, a commercial receiver (NovAtel's Portable MEDLL Receiver) (NovAtel Inc. 2002) and an analysis tool (NovAtel Multipath Assessment Tool) (NovAtel Inc. 2001) were utilized. The existing experiment environment for the analysis of the multipath effects by NovAtel is shown in Fig. 2 (NovAtel Inc. 2001).

In the existing experiment environment, the results of multipath effect assessment to select a ground stations for GNSS, GBAS, and SBAS are assessment in MAT using the measurements of desirable and undesirable signal intensities provided by MEDLL receiver. However, KASS project started since 2014 cannot perform the same effect assessment due to the discontinued equipment of NovAtel. In this study, a multipath error estimation algorithm was developed for multipath effect assessment and K-MAT was implemented to replicate the results. The multipath error estimation was conducted by removing the error contained in the measurement model equation through linear combination between dual frequency measurements, and the same results with that was replicated in the MAT.

3. ESTIMATION OF THE MULTIPATH ERROR

The pseudorange model equations based on L1/L2 dual frequency signal code and carrier phase for multipath error estimation are presented in Eqs. (2-5) (Weiss 2007).

$$P^{L1}(t) = R(t) + I^{L1}(t) + T(t) + MP^{L1}(t) + NP^{L1}(t) \quad (2)$$

$$\Phi^{L1}(t) = R(t) - I^{L1}(t) + T(t) + M\Phi^{L1}(t) + \lambda^{L1}A^{L1}(t) + N\Phi^{L1}(t) \quad (3)$$

$$P^{L2}(t) = R(t) + I^{L2}(t) + T(t) + MP^{L2}(t) + NP^{L2}(t) \quad (4)$$

$$\Phi^{L2}(t) = R(t) - I^{L2}(t) + T(t) + M\Phi^{L2}(t) + \lambda^{L2}A^{L2}(t) + N\Phi^{L2}(t) \quad (5)$$

Here, $P(t)$ is a code-based pseudorange, $\Phi(t)$ is a carrier phase-based pseudorange, $R(t)$ is a geometric distance, $I(t)$ is the ionospheric delay, $T(t)$ is a tropospheric delay, $MP(t)$ is a multipath error of code-based pseudorange, $M\Phi(t)$ is a multipath error of carrier phase-based pseudorange, $NP(t)$ is receiver noise from the code-based pseudorange, $N\Phi(t)$ is receiver noise from the carrier phase-based pseudorange, λ is a wavelength of the center frequency, and $A(t)$ is the integer ambiguity of the carrier phase measurement. L1/L2 refer to signals whose center frequency is 1575.42 MHz and 1227.6 MHz, respectively (Misra & Enge 2006).

In this study, for the use of ionospheric error removal model, receiver noise filtering, and calculation of means and elimination of float ambiguity were conducted to estimate the multipath error ($MP(t)$) contained in the code-based pseudorange. The ionospheric error was calculated by Eq. (6), applying the ionospheric free model (Misra & Enge 2006) that reflected the ionospheric error characteristics according to the carrier wave center frequency.

$$\Phi^{L1-L2}(t) = I^{L2-L1}(t) + \lambda^{L1}A^{L1}(t) - \lambda^{L2}A^{L2}(t) + M\Phi^{L1-L2}(t) + N\Phi^{L1-L2}(t) \quad (6)$$

Here, $L1$-$L2$ refers to an operator that subtracts $L2$ frequency measurement from $L1$ frequency measurement, and if Eq. (6) is rearranged under the same assumption of Eq. (7), it can be approximated as Eq. (8).

$$I^{L2-L1}(t) + \lambda^{L1}A^{L1}(t) - \lambda^{L2}A^{L2}(t) \gg M\Phi^{L1-L2}(t) + N\Phi^{L1-L2}(t) \quad (7)$$

$$\Phi^{L1-L2}(t) \approx I^{L2-L1}(t) + \lambda^{L1}A^{L1}(t) - \lambda^{L2}A^{L2}(t) \quad (8)$$

If Eq. (8) is rearranged from the propagation delay relationship ($\alpha=I^{L2}/I^{L1}=(f^{L1}/f^{L2})^2$) in the ionosphere, it can produce the ionospheric error of $L1$ signal, which is presented in Eq. (9). Here, f^{L1} and f^{L2} are the center frequencies of $L1$ and $L2$ signal (Misra & Enge 2006).

$$I^{L1}(t) \approx \Phi^{L1-L2}(t)/(\alpha-1) + [\lambda^{L2}A^{L2}(t) - \lambda^{L1}A^{L1}(t)]/(\alpha-1) \quad (9)$$

The difference measurement of the code and carrier phase-based pseudorange, which is to remove the tropospheric error contained in the code and carrier phase-based pseudorange in common, can be expressed as Eq. (10) (Weiss 2007).

$$P^{L1}(t) - \Phi^{L1}(t) = 2 \times I^{L1}(t) + [MP^{L1}(t) + NP^{L1}(t)] - [M\Phi^{L1}(t) + N\Phi^{L1}(t)] - \lambda^{L1}A^{L1}(t) \quad (10)$$

Here, since the multipath error contained in the carrier phase-based pseudorange is much smaller than that contained in the code-based pseudorange $\{[MP^{L1}(t)+NP^{L1}(t)] \gg [M\Phi^{L1}(t)+N\Phi^{L1}(t)]\}$, Eq. (10) can be rearranged to Eq. (11) (Weiss 2007).

$$P^{L1}(t) - \Phi^{L1}(t) \approx 2 \times I^{L1}(t) + [MP^{L1}(t) + NP^{L1}(t)] - \lambda^{L1}A^{L1}(t) \quad (11)$$

If the ionospheric error Eq. (9) is subtracted from Eq. (11), which removes the tropospheric error contained in the L1 code-based pseudorange, it produces Eq. (12).

$$[MP^{L1}(t) + NP^{L1}(t)] - \left[\lambda^{L1}A^{L1}(t) - \frac{2\alpha}{\alpha-1}\right] \approx P^{L1}(t) - \Phi^{L1}(t)\left[\frac{2}{\alpha-1}+1\right] + \Phi^{L2}(t)\left[\frac{2}{\alpha-1}\right] \quad (12)$$

In order to remove $NP^{L1}(t)$ from Eq. (12), moving average filtering (MAF) whose mean section is 600 sec (2q-1) is performed with regard to the receiver noise characteristics under the assumption of white Gaussian distribution to produce Eq. (13) (Misra & Enge 2006).

$$MP^{L1}(t) - \left[\lambda^{L1}A^{L1}(t) - \frac{2\alpha}{\alpha-1}\right] \approx \frac{1}{2q-1}\sum_{t=-q}^{q}\left\{P^{L1}(t) - \Phi^{L1}(t)\left[\frac{2}{\alpha-1}+1\right] + \Phi^{L2}(t)\left[\frac{2}{\alpha-1}\right]\right\} \quad (13)$$

Since the integer ambiguity is maintained at the continuous section (where no cycle slip occurs), float ambiguity ($A^{L1}(t)$) is calculated from the mean of MAF measurements in the continuous section. The multipath error of the final code

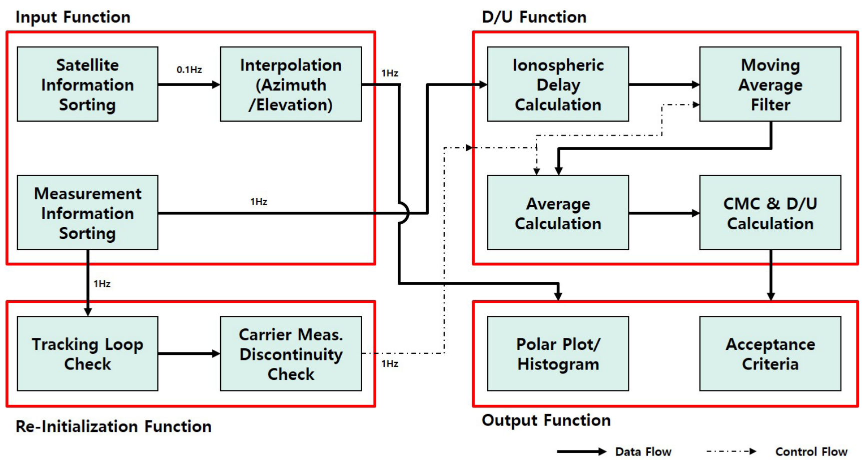

Fig. 3. K-MAT block diagram & parameter flow.

pseudorange can be estimated using Eq. (14).

$$MP^{L1}(t) \approx \frac{1}{2q-1}\sum_{t=-q}^{q} \left\{P^{L1}(t) - \Phi^{L1}(t)\left[\frac{2}{\alpha-1}+1\right] + \Phi^{L2}(t)\left[\frac{2}{\alpha-1}\right]\right\} + \left[\lambda^{L1}A^{L1}(t) - \frac{2\alpha}{\alpha-1}\right] \quad (14)$$

4. DEVELOPMENT OF K–MAT

K-MAT replicates the multipath assessment results after receiving the log files provided by commercial receivers as an input data. K-MAT consists of input function, re-initialization function, D/U function, and output function. The variables of K-MAT are divided into data and control variables. The data variables, which are variables to calculate D/U values, include pseudorange, visible satellite information (elevation, azimuth angle), and internally calculated information in K-MAT. The control variables are variables required to calculate filtering and MAF parameters, and include quality information (tracking status, carrier phase pseudorange cycle slip) of receivers and measurements. Fig. 3 shows the block diagram of K-MAT and flow of variables (data and control variables).

For the input function, satellite information (GPS time, GPS pseudorandom noise (PRN) number, and GPS satellite elevation/azimuth) and measurement information (L1/L2 code pseudorange, L1/L2 carrier phase pseudorange, and code/carrier tracking status) are extracted from binary log files provided by receivers. Since the collection interval between satellite information and measurement information provided by receivers was different, satellite information was interpolated between 0.1 Hz and 1 Hz to make the collection interval the same.

The re-initialization function determines discontinuity of carrier phase pseudorange and receiver tracking status. It creates control variables which will be used in the D/U function. The receiver tracking status is determined by checking the tracking information status values for each satellite provided by receivers to ensure the reliability of the pseudo range measurement. The discontinuity of the carrier phase pseudorange verifies whether a cycle slip occurs based on the threshold determination using time difference value of the carrier phase measurements. It determines the calculation section of float ambiguity means.

The D/U function estimates multipath errors contained in the code pseudorange from the float ambiguity means, filtering, and linear combination using raw pseudorange measurements. The multipath error estimation is implemented by discretization of the equations presented in Chapter 3. The ionospheric delay calculation provides the ionospheric free model (Misra & Enge 2006) using the signal delay characteristics. The MAF provides filtered results assuming that receiver noise follows the white Gaussian distribution. The average calculation computes a mean of float ambiguity contained in the code and carrier difference model equation in the continuous section to remove the carrier float ambiguity. It confirmed the multipath affection using the code-minus-carrier phase (CMC) and D/U. In this study, the relationship between CMC and D/U is defined by the K-factor, and additional studies on the relationship will be conducted in future. The K-factor in the currently developed K-MAT was defined as 1 and implemented to be changeable by future users.

The output is divided into a polar plot for directivity analysis on multipath effects, histograms for statistical analysis, and acceptance criteria. The polar plot replicates the largest D/U value (worst multipath error) in a unit cell (azimuth interval: 10-degree, elevation interval: 5-degree) according to azimuth and elevation values. The histogram replicates overall distribution of D/U values. Acceptance criteria provide whether D/U values of the received signals at GNSS antennas

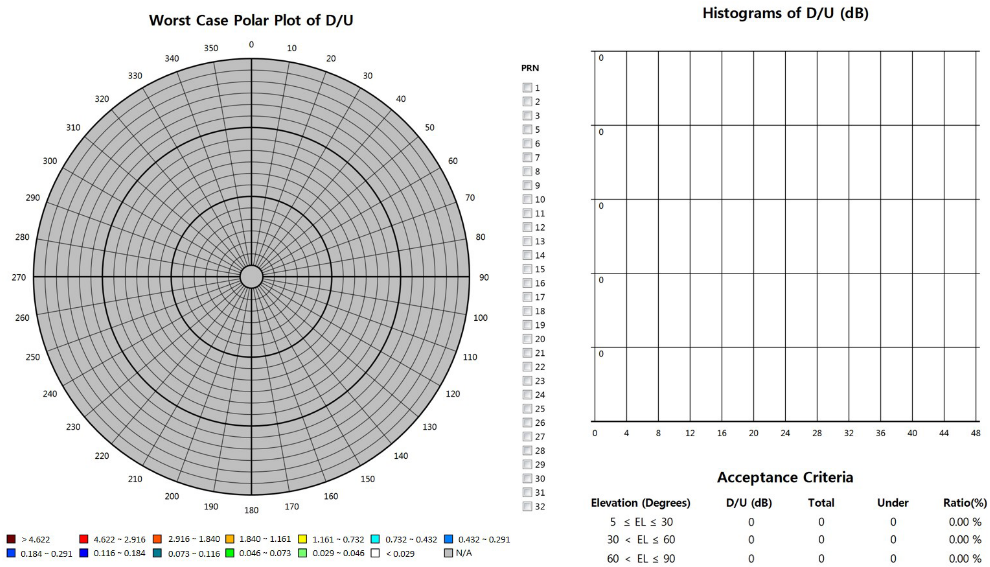

Fig. 4. KASS multipath assessment tool GUI.

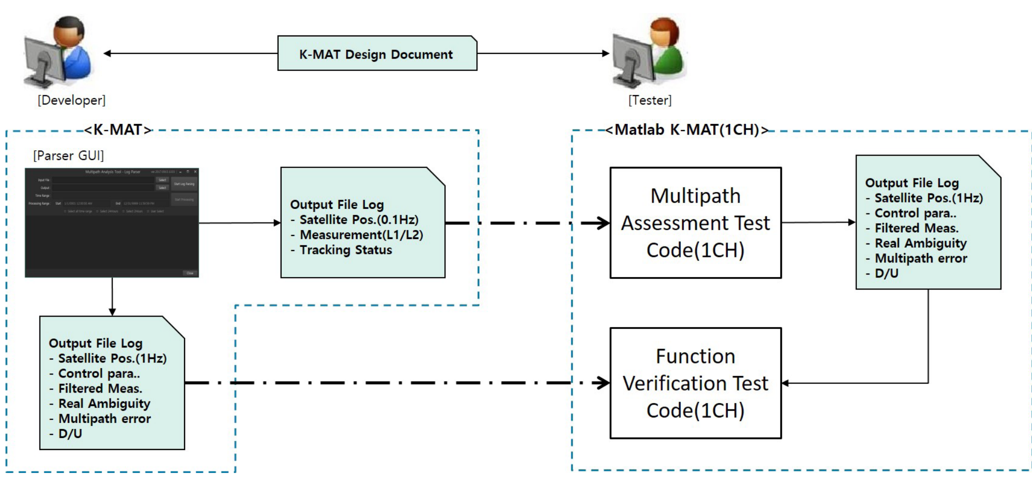

Fig. 5. K-MAT functional test (black box test).

satisfy the criteria based on the D/U threshold value selected in the site requirements. The result graphic user interface provided by the output in K-MAT is shown in Fig. 4.

5. VERIFICATION

This study conducted function tests of specification-based technique by the third party (tester) and performance tests in an known position that can predict the multipath effects to verify the developed K-MAT.

5.1 Function Test

For the function test, black box tests were conducted with regard to a single channel of K-MAT. The black box test verifies whether correct outputs are produced in response to correct inputs based on input/output test cases (Khan 2011). In this study, test cases were created by the tester using the measurements provided by real GNSS as input values. For the expected output values in the test cases, data variables (interpolated satellite position, filtered measurements, float ambiguity, multipath error, and D/U) generated from the four functions and control variables (tracking status and carrier phase measurement interruption) were selected. The function test of K-MAT was conducted by the third party (tester) and the environment for the function test is shown in Fig. 5.

For the inputs in the test cases, GNSS measurements of single GPS satellite (same PRN) provided by a 24-hour commercial receiver were collected. A tester implemented

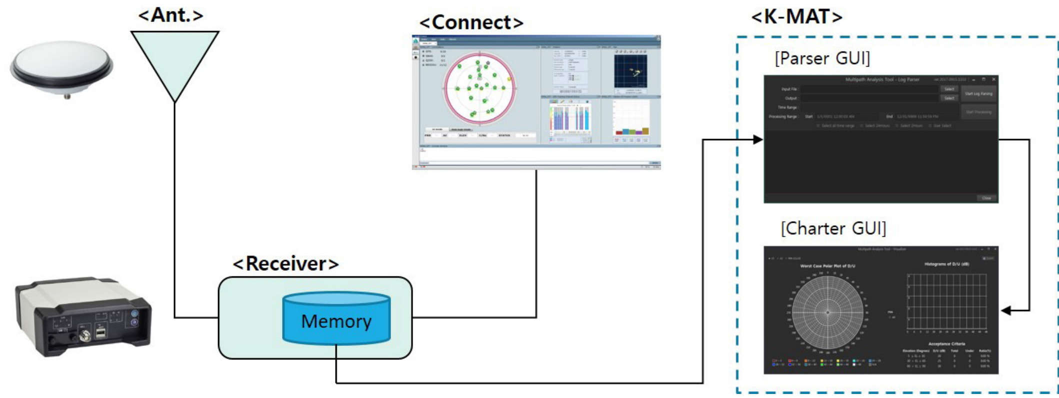

Fig. 6. Experiment environment.

software that had a single channel to create the expected output value of the variables generated by the four functions. The expected output values generated by the tester were verified through comparison with the output values of K-MAT in the function verification test code. The results were verified that the expected output values were the same with the output of K-MAT except for numerical errors (errors to six decimals under) due to the difference between software development tools. Since the numerical errors of K-MAT did not affect the multipath effect analysis results, the K-MAT function test can be verified that there was no error.

5.2 Performance Test

In the performance test, data were collected for 24 hours and performance results were compared with multipath assessment results of K-MAT through the multipath effect prediction due to surrounding geographic features, which were similar to actual environment for multipath assessment. In this study, experiment environment was configured using multi GNSS receiver antenna (VEXXIS TM GNSS-850) (NovAtel Inc. 2017a) and multi GNSS receivers (ProPak 6TM, OEM 638) (NovAtel Inc. 2017b) of NovAtel, and GPS raw measurements were collected. The experiment environment (antenna, receiver, connecting software, and K-MAT) for data collection is shown in Fig. 6.

The GNSS receiver used in the site investigation was set to a narrow correlator, and measurement setup values of code and carrier phase are presented in Table 1. The GNSS receiver setup was the same with that of the receiver (NovAtel G-III Receiver), which will be used in KRS in future. The log files stored inside the GNSS receiver are satellite information and raw data, which are set as presented in Table 2.

The binary log files stored in the internal memory of GNSS receiver perform multipath assessment through external storage and the results are placed in K-MAT. The

Table 1. GNSS receiver configuration setting & command.

	Configuration setting	Command
L1 Measurement	Non Smoothed Code	DLLTIMECONST GPSL1CA 0
	PLL BANDWITH (10 Hz)	PLLBAND WIDTH GPSL1CA 10
L2 Measurement	Non Smoothed Code	DLLTIMECONST GPSL2P 0
	PLLBANDWITH (10 Hz)	PLLBAND WIDTH GPSL2P 10

Table 2. GNSS message logging type & command.

	Message logging type	Command
Satellite Information	SATVIS LOG (0.1 Hz)	LOG FILE SATVISB ONTIME 10
Raw Measurement	RANGE LOG (1 Hz)	LOG FILE RANGEB ONTIME 1

performance tests in actual environment employed the same configuration in Fig. 6, and GPS raw measurements were collected for 24 hours at the rooftop in the Korea Aerospace Research Institute. The left figure in Fig. 7 expresses short-range targets (steel and concrete structures, indicated by blue circle) and long-range targets (hills, marked by green area) with regard to objects whose height is higher than the height of antenna (marked as white triangle). The right figure in Fig. 7 shows the multipath assessment results according to the surrounding structures and hills around the antenna.

The multipath assessment results verified that signals were not processed in the direction where GNSS signals could not be received, which was not included in GPS operation orbit, in the direction between ±30-degrees on the basis of the 360-degree azimuth of the polar plot. In addition, the results using GPS visibility analysis tool (PEGASUS) in the direction between 170 to 180-degree azimuth verified that signals were not collected in the direction where GPS signals were not received in Korea at the time of the measurements. Mostly in the west, low mountains were formed long distance (within 100 m), so GPS signals cannot be received at low elevation (0° to 5°) and the effect of the multipath signals occurred in most of the cells (yellow region, multipath error: within 1.16 m) at the elevation of 5° to 30°. The effect of the multipath signals was occurred in some cells due to the objects (azimuth: 35°, 140°, and 250°) located within a short distance (less than 15 m)

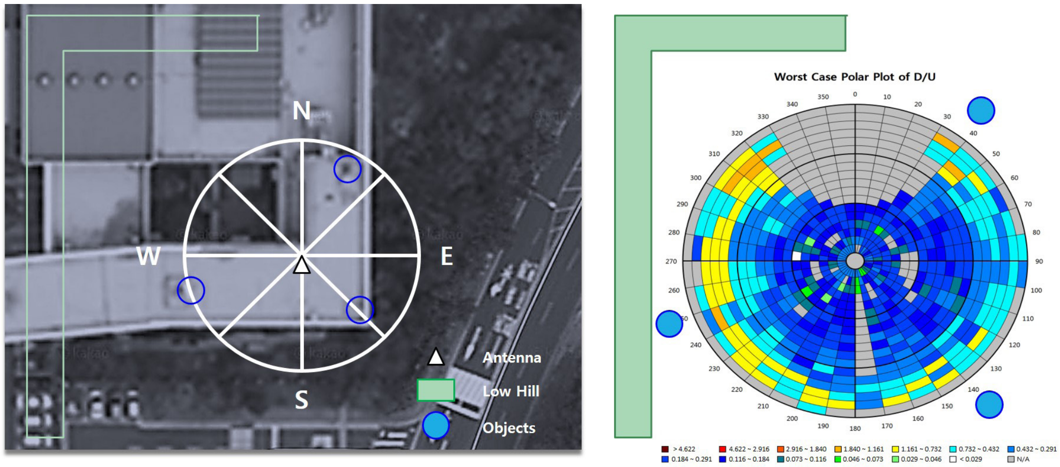

Fig. 7. Multipath assessment using the real data at the rooftop (left: multipath objects, right: multipath assessment result).

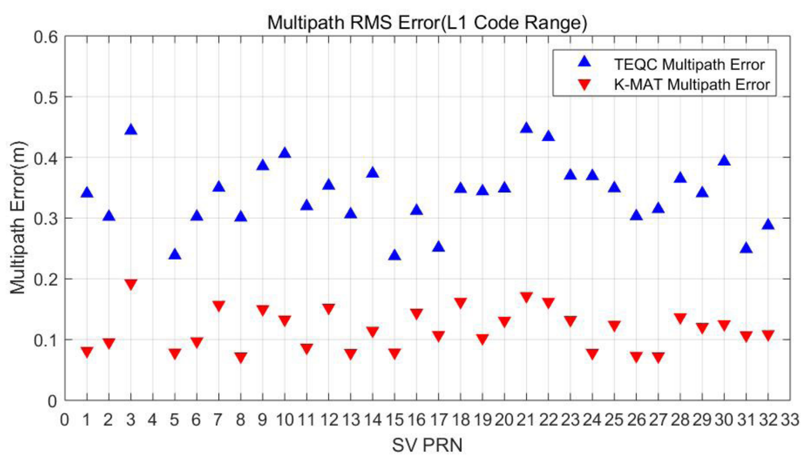

Fig. 8. L1 C/A code pseudorange multipath error.

from the antenna (orange region, multipath error: within 1.84 m). The performance test results verified that the multipath effect predicted according to the distance between antenna and geographic feature. The K-MAT results were similar. Furthermore, the TEQC software used in the performance test was a tool for the quantitative comparison of GNSS data, which analyzed GNSS measurement performance using RINEX data. The results by the software TEQC (UNAVCO 2014) that provided multipath errors contained in the code pseudorange for each satellite and K-MAT performance results were compared. Fig. 8 shows the comparison results.

The multipath error mean by satellite was difficult to be compared numerically but the relative error characteristics were verified to have a mean value within 0.2 m. The numerical comparison is meaningful in performance analysis under the same algorithm conditions. However, since this study identified multipath direction where multipath errors occurred using the developed tools for the purpose of site investigation, selected optimum antenna locations, and eliminated the obstacles, the relative error between the tools is not a serious problem.

6. CONCLUDING REMARKS AND FUTURE WORK

This study developed and verified the KASS multipath assessment tool (K-MAT) using the multipath error estimate contained in the code pseudorange to replace the existing commercial equipment only for the multipath assessment. The multipath error algorithm eliminated the ionospheric and tropospheric delay errors through difference technique between L1/L2 codes and carrier phase pseudorange measurements, as well as receiver noise and float ambiguity by the measurement characteristics. The functions of K-MAT were defined and implemented as they were divided into four functions. In particular, the multipath assessment converted the results into D/U values which were used in existing commercial analysis tool (MAT) and displayed the result with polar plots and histograms. The function and performance tests of the implemented K-MAT were conducted by the third party (tester) at a real environment. In the function test, tester generated test cases for black box tests with regard to a single satellite channel, and K-MAT outputs and expected output values were compared for verification purpose. In the performance test, GPS raw measurements were collected for 24 hours, and predictable multipath effects were compared and analyzed with K-MAT results for verification.

The K-MAT is an important tool for surrounding environmental investigation around the antennas, which will be utilized in precision investigation for site selection of ground infrastructure facilities (reference station, satellite communication stations, and integrated operation stations). Furthermore, the developed algorithm will be applied to various multipath error estimation algorithms that were previously studied, thereby conducting studies on improvement of multipath assessment accuracy of K-MAT continuously.

ACKNOWLEDGMENTS

This research was part of the project titled 'Development of Multi-purpose Reference Technologies for Augmentation System', funded by the Ministry of Oceans and Fisheries, Korea.

REFERENCES

Cho, S. L., Jang, H. J., Son, M. H., Lee, J. E., Park, T., et al. 2017, A Study on the Multipath Effect of Infrastructure for KASS Reference station, 2017 KGS Conference, Jeju, Korea, 1-3 November 2017, pp.321-324

Jakab, A. & Townsend, B. 2001, Analysis of the Multipath Meter Performance in the presence of Anomalous Satellite Signals, Proceedings for the Institute of Navigation, January 2001, pp.541-551

Khan, M. E. 2011, Different Approaches to Black Box Testing Technique finding errors, International Journal of Software Engineering & Application (IJSEA), 2(4), October 2011. https://doi.org/10.5121/ijsea.2011.2404

Misra, P. & Enge, P. 2006, Global Positioning System: Signal, Measurements and Performance, 2nd ed. (Lincoln, MA: Ganga-Jamuna Press)

NovAtel Inc. 2001, Multipath Assessment Tool, (MAT) User Manual, available from: http://www.sokkiatopcon.tw/NONATEL/ /Documents/Manuals/om-200000054.pdf

NovAtel Inc. 2002, PORTABLE MEDLL RECEIVER, Installation and Operation Manual, available from: https://www.novatel.com/assets/Documents/Manuals/om-200000065.pdf

NovAtel Inc. 2017a, VEXXISTM Antennas GNSS-850, Cutting edge antenna technology with superior tracking performance, available from: https://www.novatel.com/assets/Documents/Papers/GNSS-850-Product-Sheet.pdf

NovAtel Inc. 2017b, ProPak6TM, Installation & Operation User Manual, available from: https://www.novatel.com/assets/Documents/Manuals/OM-200000148.pdf

Townsend, B., Wiebe, J., Jakab, A., Clayton M., & Murfin, T. 2000, Analysis of the Multipath Meter Performance in Environments with Multiple Interferers, ION GPS 2000, Salt Lake City, UT, 20-22 Sep. 2000

UNAVCO 2014, Teqc Tutorial: Basics of Teqc use and Teqc Products, available from: https://www.unavco.org/software/data-processing/teqc/doc/UNAVCO_Teqc_Tutorial.pdf

Weiss, J. P. 2007, Modeling and Characterization of Multipath in Global Navigation Satellite System Ranging Signals, Doctor's Degree, University of Colorado, USA

Yun, Y. S., Lee, E. S., Heo, M. B., & Nam, G. W. 2016, KASS Message Scheduler Design, Journal of Positioning, Navigation, and Timing, 5, 193-202. https://doi.org/10.11003/JPNT.2016.5.4.193

SungLyong Cho received the B.S. and Ph.D. degree in the Department of Electronics Engineering from Chungnam National University, Korea in 2007 and 2015, respectively. He is now working in Korea Aerospace Research Institute. His research interests include Precise positioning system, SBAS Safety & GNSS measurement analysis (Multipath Error) technologies.

ByungSeok Lee received the B.S. and Ph.D. degree in the Department of Electrical and computer Engineering from University of Seoul, Korea 2002 and 2015, respectively. He is now working in Korea Aerospace Research Institute. His research interests include system control, SBAS system engineering technologies.

JongYeoun Choi received the B.S and M.S. degree in the Department of Electronics Engineering from Kyungpook National University, Korea in 1992 and 1995, respectively. And he received his Ph.D. degree in the Department of Electronics Engineering from Chungnam National University, Korea in 2011. He is now working in Korea Aerospace Research Institute. His research interests include satellite & KASS system engineering technologies.

GiWook Nam received a B.S. in aeronautical science & flight operation and M.S. in aeronautical engineering from Korea Aerospace University, South Korea, in 1983 and 1988, respectively. And he received his Ph.D. degree in aerospace system design from the College of Aeronautics, Cranfield University, U.K., in 1997. He is currently a head of SBAS program office and the Satellite Navigation ·Application Technology R&D Center at the Korea Aerospace Research Institute, South Korea. He works on global navigation satellite systems and system safety.